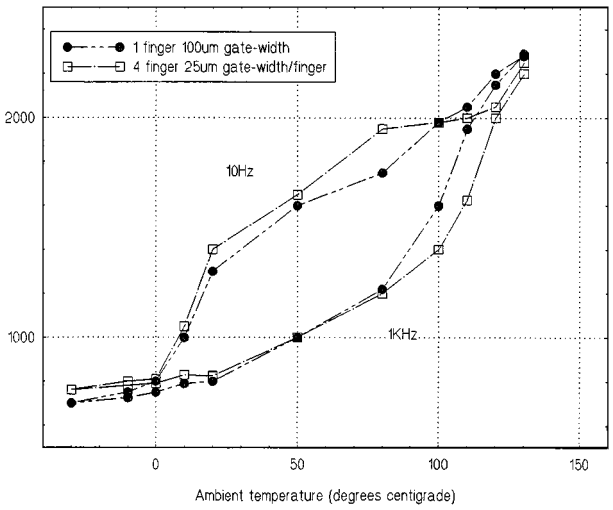

Fig. 9. Drain–source resistance for 100-μm devices composed of 1–4 fingers.

off (as in Fig. 3) as a function of ambient temperature. This enables the dependency of the dispersion effect on ambient temperature to be determined over a wide temperature range without the complications introduced by the static bias. The results of this are summarized in Fig. 8, which shows the drain–source resistance before (at 10 Hz) and after (at 1 kHz) the frequency-disperison effect. This data was measured from the static point of $V_{\rm GS} = 0$ V, $V_{\rm DS} = 0$ V by pulsing the drain terminal only and corresponds to the $v_{\rm gs} = 0$ V, $v_{\rm ds} = 2$ V dynamic point. The corresponding information for smaller devices is shown in Fig. 9 to illustrate the fact that under high- and low-temperature conditions, the device becomes free of the dispersion effect. This occurs because of the change in the Fermi level as the temperature is varied. This facilitates the release of electrons from the traps under high-temperature conditions and exhibits the process as the temperature and the Fermi level is lowered. The information in Fig. 9 clearly shows the significant effect that the number of fingers has on the thermal and dispersion characteristics of the device. The thermal impedance for the one-finger device was measured as 270 °C/W, whereas for the four-finger device, the value is 333 °C/W.

VII. Conclusions

A measurement system for quantifying the dependency of the frequency-disperison effect on electric field and temperature has been presented. This uses a pulsed IV measurement system and a thermally controlled wafer prober. The pulsed measurements can be performed by pulsing either the gate or drain or both terminals. The results presented indicate that the differences observed between the static and dynamic characteristics are to a significant extent due to frequency-disperison effects.

Pulsed IV measurements carried out in conjunction with liquid crystals show that a relatively long pulsewidth (approximately 10 ms) is required before the self-heating effect has a measurable effect on the IV characteristics of a medium-size power transistor.

References

[1] J. Rodriguez-Tellez, B. P. Stothard, and M. Al-Daas, "Static, pulsed and frequency-dependent IV characteristics of GaAs FETs," *Proc. Inst. Elect. Eng.*, pt. G, vol. 143, pp. 129–133, June 1996.

[2] ——, "Frequency and temperature dependency of output conductance of GaAs FETs," *Microwave J.*, vol. 38, no. 8, pp. 88–94, Aug. 1995.

[3] J. M. Golio, M. G. Miller, G. N. Maracas, and D. A. Johnson, "Frequency-dependent electrical characteristics of GaAs MESFETs," *IEEE Trans. Electron Devices*, vol. 37, pp. 1217–1227, May 1990.

[4] T. Fernandez, Y. Newport, J. M. Zamarillo, A. Mediavilla, and A. Tazon, "High-speed automated pulsed IV measurement system," in *23rd European Microwave Conf.*, Madrid, Spain, Sept. 1993, pp. 494–496.

[5] J. Rodriguez-Tellez, S. Laredo, and R. W. Clarke, "Self-heating in GaAs FETs—A problem?," *Microwave J.*, vol. 37, no. 9, pp. 76–92, Sept. 1994.

[6] J. A. Higgins, "Thermal properties of power HBTs," *IEEE Trans. Electron Devices*, vol. 40, pp. 2171–2177, Dec. 1993.

[7] J. P. Teyssier, P. Bouysse, Z. Ouarch, D. Barataud, T. Peyretaillade, and R. Quere, "40-GHz/150-ns versatile pulsed measurement system for microwave transistor isothermal characterization," *IEEE Trans. Microwave Theory Tech.*, vol. 46, pp. 2043–2052, Dec. 1998.

[8] A. E. Parker and J. B. Scott, "Method for determining correct timing for pulsed *I/V* measurement of GaAs FETs," *Electron. Lett.*, vol. 31, pp. 1697–1698, Sept. 1995.

Numerical Investigation of the Field and Current Behavior Near Lossy Edges

Marco Farina and Tullio Rozzi

***Abstract*—Real circuits involve metallic edges with finite conductivity and nonideal dielectrics. Usually it is more or less implicitly assumed that fields and induced currents behave as if conductors and dielectrics were ideal. In this paper, we show that this assumption is partially erroneous and that the presence of real conductors and dielectrics seems to lead to a simpler and more physical picture, where longitudinal currents are shown to be nonsingular.**

***Index Terms*—Coplanar waveguides, lossy circuits, Maxwell's equations, numerical analysis, wedges.**

I. Introduction

Wedges are sometimes more than a purely academic concern, as recently shown by several authors. In fact, while on the one hand, the knowledge of the field behavior near wedges may be used *a posteriori* in order to check the consistency of numerical solutions, it may be also introduced *a priori* in the numerical solution of integral equations in order to speed up its rate of convergence [1], [2].

Sharp edges are frequently encountered in practice, and, as their sharpness is assumed to be infinite, they may induce singularities in fields and source densities. If, from a theoretical point-of-view, the correct singularity conditions are needed in order to ensure the uniqueness of the field solution [3], in many practical cases, it is just sufficient to have an estimate of the field behavior in order to substantially increase the speed and accuracy of numerical algorithms. This is particularly true when dealing with massively numerical techniques, such as finite differences (FDs) or transmission line methods (TLMs), where the whole space of the analyzed structure has to be cleverly discretized. In these methods, sharp variations in the field would require either great over-meshing or a more expedient inclusion *ab initio* of the known field behavior in the formulation itself. The latter strand is very

Manuscript received February 4, 2000; revised October 10, 2000.

The authors are with the Dipartimento di Eletronnica ed Automatica, Universita degli Studi di Ancona, 60131 Ancona, Italy.

Publisher Item Identifier S 0018-9480(01)05064-5.

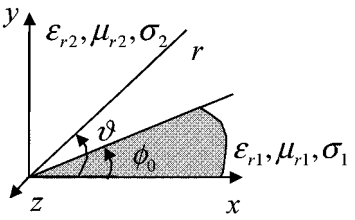

Fig. 1. Nonideal dielectric wedge, infinite in the z-direction.

attractive, as it allows obtaining greater accuracy without paying for additional computational load, and has been successfully followed both for the finite-difference time-domain (FDTD) [4]–[7] and the TLM [8] approaches.

There is a wealth of references concerning singularity conditions in proximity of ideal dielectric and ideal conducting wedges; a long list may be found in [1], [2]. Nonetheless, just a few papers addressed the topic of the field behavior near nonideal edges, e.g., [9] and [10].

The aim of this paper is to provide a full-wave numerical investigation of the field behavior near the edges in "real" structures, considering, in particular, a conductor-backed coplanar waveguide (CPW) and a microstrip with lossy thick conductors. Nevertheless, an attempt is also made to draw some analytical conclusions by inspection of Maxwell's equations.

II. Theory—2-D Edges

It is possible to get some theoretical insights about the field behavior near lossy conductors in the particular case of a two-dimensional (2-D) edge, by retracing the line of reasoning usually followed when treating dielectric wedges [11], but considering now a complex permittivity.

To this aim, let us consider Fig. 1, which shows a wedge between two linear, isotropic, and homogeneous media: the edge is "sharp," having a zero radius of curvature, and infinite in the z-direction.

Fields are expressed by using Hertzian potentials in a cylindrical coordinate system. Assuming z-oriented electric and magnetic potentials, one obtains

$$\begin{aligned} E_z &= \omega^2 \mu \varepsilon_0 \kappa(\omega) \psi_e \\ H_z &= \omega^2 \mu \varepsilon_0 \kappa(\omega) \psi_h \\ E_r &= -j \frac{\omega \mu}{r} \partial_\vartheta \psi_h \\ H_r &= j \frac{\omega \varepsilon_0 \kappa(\omega)}{r} \partial_\vartheta \psi_e \\ E_\vartheta &= j \omega \mu \partial_r \psi_h \\ H_\vartheta &= -j \omega \varepsilon_0 \kappa(\omega) \partial_r \psi_e. \end{aligned} \tag{1}$$

In the above expressions, we have focused waves uniform in just the z-direction. This assumption allows to set to zero all z-derivatives, thus reducing the general problem to a 2-D one. Note that, due to the 2-D assumption, none of the fields in (1) involves E and H potentials at the same time: the fields originated are purely TM and TE, and TM and TE fields may be considered separately.

Both potentials have to satisfy the Helmholtz equation in each region, namely,

$$\nabla^2 \psi + k^2 \psi = 0. \tag{2}$$

Near the edges, however, the condition holds

$$\nabla^2 \gg k^2 \tag{3}$$

namely, the spatial variations are sharper than the frequency ones. This noteworthy property allows approximating the potentials by the solutions of Laplace's equation that are the quasi-static solutions.

One should bear in mind, however, that, in the lossy case, frequency plays an important role anyway, by determining to what extent the material behaves as a dielectric or conductor; hence, all the quantities involved are frequency dependent, while satisfying the Laplace equation.

Hence, the possible solutions are

$$\begin{aligned} \psi_{e,h}^{(1)}(\vartheta, r) &= r^\nu \left[A_{e,h}^{(1)} \sin(\nu\vartheta) + B_{e,h}^{(1)} \cos(\nu\vartheta) \right] \\ \psi_{e,h}^{(2)}(\vartheta, r) &= r^\nu \left[A_{e,h}^{(2)} \sin\left[\nu(\vartheta - \phi_0)\right] + B_{e,h}^{(2)} \cos\left[\nu(\vartheta - \phi_0)\right] \right] \end{aligned} \tag{4}$$

where the apex refers to the region, while A and B are unknown coefficients. In our case, ν is generally complex, and just its real part contributes to the singularity.

Tangential field continuity must be ensured at each interface so that

$$\begin{aligned} E_z^{(1)}(0, r) &= E_z^{(2)}(2\pi, r) \\ E_r^{(1)}(0, r) &= E_r^{(2)}(2\pi, r) \\ H_z^{(1)}(0, r) &= H_z^{(2)}(2\pi, r) \\ H_r^{(1)}(0, r) &= H_r^{(2)}(2\pi, r) \\ E_z^{(1)}(\phi_0, r) &= E_z^{(2)}(\phi_0, r) \\ E_r^{(1)}(\phi_0, r) &= E_r^{(2)}(\phi_0, r) \\ H_z^{(1)}(\phi_0, r) &= H_z^{(2)}(\phi_0, r) \\ H_r^{(1)}(\phi_0, r) &= H_r^{(2)}(\phi_0, r) \end{aligned} \tag{5}$$

for arbitrary r. The above set of conditions leads to a homogeneous system. Seeking for nontrivial solutions of the determinants

$$\begin{aligned} \Delta_h(\nu) = {} & 2\kappa_1\kappa_2 \left[1 - \cos(\nu\phi_0) \cos\left(\nu(\phi_0 - 2\pi)\right) \right] \\ & - \left(\kappa_1^2 + \kappa_2^2\right) \left[\sin(\nu\phi_0) \sin\left(\nu(\phi_0 - 2\pi)\right) \right] \\ = {} & 0 \\ \Delta_e(\nu) = {} & 2\mu_1\mu_2 \left[1 - \cos(\nu\phi_0) \cos\left(\nu(\phi_0 - 2\pi)\right) \right] \\ & - \left(\mu_1^2 + \mu_2^2\right) \left[\sin(\nu\phi_0) \sin\left(\nu(\phi_0 - 2\pi)\right) \right] \\ = {} & 0 \end{aligned} \tag{6}$$

for TE and TM waves, respectively, the lowest order zero will provide the order of singularity whenever $\mathrm{Re}(v)$ ranges from zero to one. What is apparent is that the TM wave condition does not involve permittivity or conductivity. Field components H_r and H_θ are singular only if $\mu_1 \neq \mu_2$ and regular for dielectric or nonideal conductor wedges. On the other hand, the tangential magnetic field is discontinuous at ideal conductors, and condition (5) must be replaced by

$$E_z^{(2)}(2\pi, r) = E_z^{(2)}(\phi_0, r) = 0 \tag{7}$$

obtaining for both TM and TE waves the well-known condition

$$\nu = \pi/(2\pi - \phi_0). \tag{8}$$

Hence, TM fields are singular just near ideal conductors and magnetic wedges, being regular in all other cases.

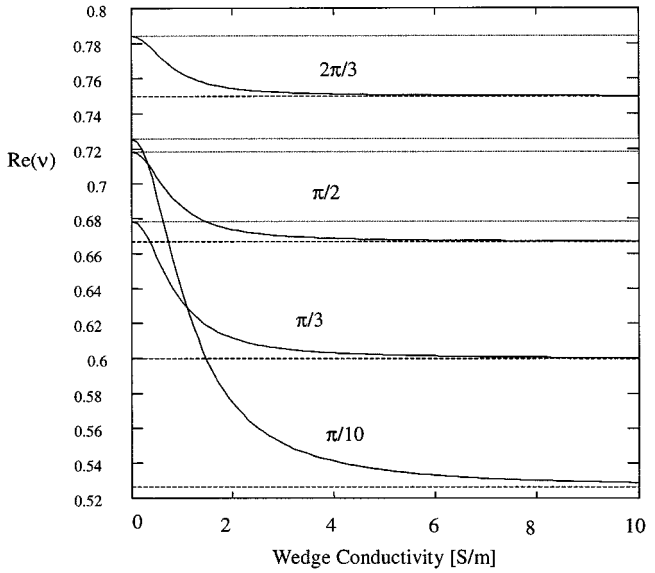

Fig. 2. Behavior of $\mathrm{Re}(\nu)$ versus the wedge conductivity for TE fields for some angles. Dashed lines represent the ideal conductor case. $\varepsilon_{r1} = 12.9$, $\varepsilon_{r2} = 1$, $f = 1$ GHz. Dotted lines represent the expected values for the ideal dielectric wedge.

On the other hand, TE fields have a smoother transition from the regular to singular condition as the conductivity is raised, and is shown in Fig. 2, where the real part of ν smoothly approaches the value expected for an ideal conductor. Fig. 3 represents the behavior of ν when both permittivity and conductivity are varied for an edge angle of $\pi/10$.

III. Theory–3-D Edges

The conclusions drawn in the previous section are strictly related to the 2-D assumption. In the general three-dimensional (3-D) case, whenever z-derivatives are not negligible, it is hard to draw analytical conclusions. Nevertheless, according to numerical simulations, some of which are reported in the following section, both magnetic- and electric-field components normal to the edge seem to be singular. This is inconsistent with the conclusion drawn for 2-D edges, where magnetic fields orthogonal to the edge just belong to TM waves and are regular. This is due to the particular decomposition in TM–TE fields occurring in the 2-D case. In general, TM and TE waves have five components of field (both have nonvanishing H_θ and H_r), and usually a singular transverse electric field would imply a singular transverse magnetic field.

In fact, if the z-derivative is not set to zero, we pose simply

$$\partial_z = -j\beta$$

and (1) is replaced by

$$\begin{aligned} E_z &= 0 \\ H_z &= \left(\omega^2\mu\varepsilon_0\kappa(\omega) - \beta^2\right)\psi_h \\ E_r &= -j\frac{\omega\mu}{r}\,\partial_\vartheta\,\psi_h \\ H_r &= -j\beta\partial_r\psi_h \\ E_\vartheta &= j\,\omega\mu\partial_r\psi_h \\ H_\vartheta &= -j\beta\frac{\partial_\vartheta\psi_h}{r} \end{aligned} \tag{9}$$

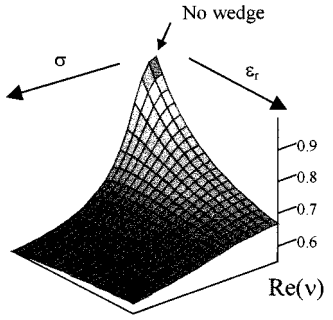

Fig. 3. Behavior of $\mathrm{Re}(\nu)$ in TE fields for varying both ε_{r1} and σ_1 assuming $\phi_0 = \pi/10$.

for TE fields and

$$\begin{aligned} E_z &= \left(\omega^2\mu\varepsilon_0\kappa(\omega) - j\beta\right)\psi_e \\ H_z &= 0 \\ E_r &= -j\beta\partial_r\psi_e \\ H_r &= j\frac{\omega\varepsilon_0\kappa(\omega)}{r}\,\partial_\vartheta\,\psi_e \\ E_\vartheta &= -j\beta\frac{\partial_\vartheta\psi_e}{r} \\ H_\vartheta &= -j\,\omega\varepsilon_0\kappa(\omega)\partial_r\psi_e \end{aligned} \tag{10}$$

for TM fields. Hence, we see, for example, that whenever E_r of a TE field is singular, H_θ ought to show the same kind of singularity, and the same kind of relationship occurs between E_θ and H_r.

This speculative reasoning does not provide us with the order of singularity; however, it gives us insight as to what to expect. As for the 2-D TE case, we expect fields near lossy conductors to behave as in proximity of ideal conductors for any reasonable conductivity value. An important question may be raised about the apparent discontinuity between conclusions obtained when ∂_z is or is not vanishing. Actually, we expect a continuous dependence of the order of singularity of the magnetic fields from ∂_z, smoothly approaching unity value for $\partial_z \to 0$, in a very similar way as shown in Fig. 3, where a smooth transition does exist when varying conductivity. A similar line of reasoning applies for the dependence by the frequency, involving a continuous transition from the dynamic to the static case.

IV. Theory—Currents

Lossy conductors may be seen just as lossy dielectrics: this obvious point-of-view leads to an interesting implication. In fact, a noteworthy property of dielectric wedges is that, unlike perfect conductors, both concave and convex edges induce field singularities. This fact is also verified by solving (6) with $\phi_0 > \pi$. However, the conductor (*volume*) currents are linked to the electric field by Ohm's law, stated proportionality between induced currents and electric fields, so that J_x and J_y have be singular and J_z has to be regular. This is a very different situation from that of an ideal conductor, where J_x and J_y (now surface current densities) are vanishing at the corner, while J_z is singular, and linked to the singularity of the magnetic-field components.

V. Numerical Results

In order to investigate numerically the field behavior near some planar structures, we have used an integral-equation approach, namely, the generalized transverse resonance-diffraction (GTRD) approach, which is extensively discussed in [12] and [13]. Fig. 4 depicts the behavior of the electric fields at the dielectric interface of a boxed

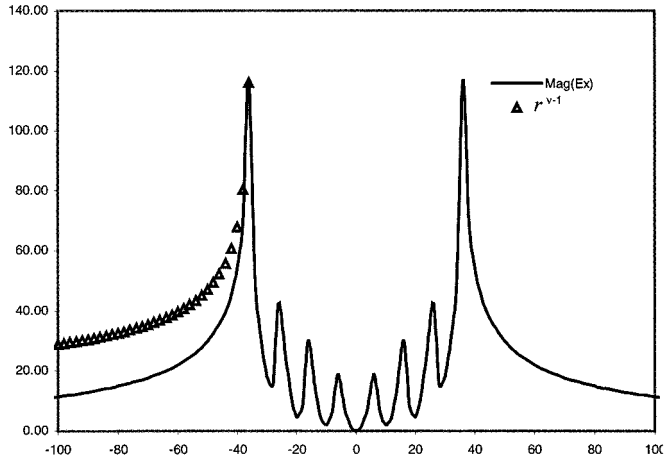

Fig. 4. Behavior of E_x on the dielectric interface of a boxed microstrip. The microstrip is 70-μm wide and 3-μm thick on a 112-μm GaAs substrate. The strip conductivity is 3 10^7 S/m.

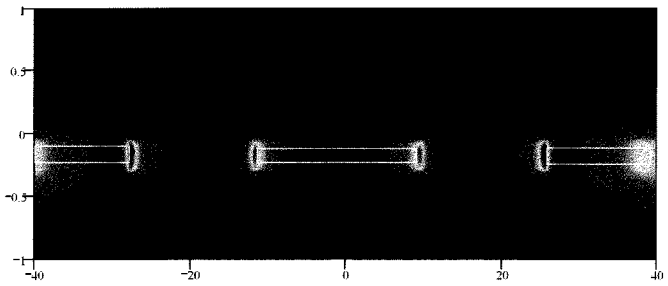

Fig. 5. Contour plot of the magnitude of H_y near electrodes of a conductor-backed CPW (dimensions not scaled).

microstrip of finite thickness and conductivity. The x-component outside the conductor ($|x| > 35$ μm) seems to follow the singular behavior expected for a perfect conductor quite well. Ripples at the conducting interface are caused by the shape and finite number of functions used to describe the conductor currents.

Fig. 5 shows the behavior of H_y in proximity of the conductors of a conductor-backed CPW for the fundamental even mode. While numerical results cannot be used to assess any singularity, it appears that H_y has at least a maximum near the edge of the conductors.

Longitudinal currents obtained from the integral equation for a lossy microstrip [14] seems to support our theory about currents. In fact, J_z follows a parabolic behavior that is extremely frequency dependent being produced by the skin effect, as it disappears at low frequencies. This is consistent with the behavior observed for E_z. On the other hand, both J_x and J_y do not ever vanish at the corners, which is consistent with the present theory.

Using a singular shape for the dominant current component, J_z generally does not produce dramatic errors in an integral approach like ours (shown in Fig. 6), where a comparison of the loss factor for a microstrip is evaluated using a single constant function, a classical $x^{0.5}$ singular function, and a piecewise constant (PWC) function; namely, a set of six subsectional constant functions. Both J_x and J_y, having a reduced impact in the simulation, are a PWC.

The computation is appositely performed at low frequencies in order to avoid the skin effect along the thickness of the strip. Using the singular function results in a shifted-up curve with respect to those obtained by a constant function, while the PWC expansion, being able

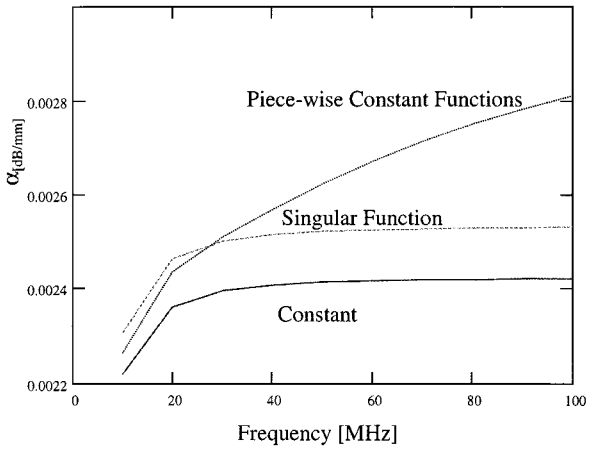

Fig. 6. Loss factor evaluated for three expanding sets of the integral equation. The microstrip is 1-mm wide and 1-μm thick. The substrate is 2-mm GaAs.

to accommodate the right frequency-dependent shape of the current, correctly models the loss factor (several validations of this set against measured data are collected in [13]). Note that, in the lower frequency range, results obtained by the PWC come close to the ones obtained by a single constant function. The upward shift induced by the assumed singular shape produces a consistent systematic error when a whole set of singular expanding functions is used.

REFERENCES

[1] J. Van Bladel, *Singular Electromagnetic Fields and Sources.* New York: Oxford, 1991.
[2] S. Marchetti and T. Rozzi, "Electric field singularities at sharp edges of planar conductors," *IEEE Trans. Antennas Propagat.*, vol. 39, pp. 1312–1320, Sept. 1991.
[3] J. Van Bladel, *Electromagnetic Fields.* New York: McGraw-Hill, 1964.
[4] G. Mur, "The modeling of singularities in the finite-difference approximation of time-domain electromagnetic-field equations," *IEEE Trans. Microwave Theory Tech.*, vol. MTT-29, pp. 1073–1077, Oct. 1981.
[5] D. B. Shorthouse and C. J. Railton, "The incorporation of static field solutions into the finite difference time domain algorithm," *IEEE Trans. Microwave Theory Tech.*, vol. 40, pp. 986–994, May 1992.
[6] P. Przybysyewski and M. Mrozowski, "A conductive wedge in Yee's mesh," *IEEE Microwave Guided Wave Lett.*, vol. 8, pp. 66–68, Feb. 1998.
[7] N. H. Huynh and W. Heinrich, "FDTD accuracy improvement by incorporation of 3-D edge singularities," in *IEEE MTT-S Int. Microwave Symp. Dig.*, June 1999, pp. 1573–1576.
[8] L. Cascio, G. Tardioli, T. Rozzi, and W. J. R. Hoefer, "A quasi-static modification of TLM at knife edge and 90° wedge singularities," *IEEE Trans. Microwave Theory Tech.*, vol. 44, pp. 2519–2524, Dec. 1996.
[9] M. Braver *et al.*, "The behavior of the electromagnetic field near the edge of a resistive half-plane," *IEEE Trans. Antennas Propagat.*, vol. 36, pp. 1760–1768, Dec. 1988.
[10] J. Geisel, K. H. Muth, K. H. , and W. Heinrich, "The behavior of the electromagnetic field at edges of media with finite conductivity," *IEEE Trans. Microwave Theory Tech.*, vol. 40, pp. 158–161, Jan. 1992.
[11] J. B. Andersen and V. V. Solodukhov, "Field behavior near a dielectric wedge," *IEEE Trans. Antennas Propagat.*, vol. AP-26, pp. 598–602, Apr. 1978.
[12] M. Farina, G. Gerini, and T. Rozzi, "Efficient full-wave analysis of stratified planar structures and unbiased TW–FET," *IEEE Trans. Microwave Theory Tech*, vol. 43, pp. 1322–1328, June 1995.
[13] T. Rozzi and M. Farina, *Advanced Electromagnetic Analysis of Passive and Active Planar Structures.* London, U.K.: IEE Press, 1999.
[14] M. Farina and T. Rozzi, "New boundary and edge conditions for real planar circuits," in *IEEE-MTT-S Int. Microwave Symp. Dig.*, vol. 3, Anaheim, CA, June 1999, pp. 1253–1256.